Inferring three-dimensional surface displacement field by combining SAR interferometric phase...

Article *in* Science China Earth Science · April 2010

DOI: 10.1007/s11430-010-0023-1

5 authors, including:

Hu Jun
Central South University

Zhiwei Li
Central South University

Zhu Jian-Jun
Central South University

Xiaoli Ding
The Hong Kong Polytechnic University

SCIENCE CHINA
Earth Sciences

• RESEARCH PAPER •

April 2010 Vol.53 No.4: 550–560
doi: 10.1007/s11430-010-0023-1

Inferring three-dimensional surface displacement field by combining SAR interferometric phase and amplitude information of ascending and descending orbits

HU Jun[1], LI ZhiWei[1*], ZHU JianJun[1], REN XiaoChong[1] & DING XiaoLi[2]

[1] Department of Survey Engineering and Geomatics, Central South University, Changsha 410083, China;
[2] Department of Land Surveying and Geo-Informatics, The Hong Kong Polytechnic University, Hong Kong, China

Received June 15, 2009; accepted November 10, 2009; published online March 3, 2010

Conventional Interferometric Synthetic Aperture Radar (InSAR) technology can only measure one-dimensional surface displacement (along the radar line-of-sight (LOS) direction). Here we presents a method to infer three-dimensional surface displacement field by combining SAR interferometric phase and amplitude information of ascending and descending orbits. The method is realized in three steps: (1) measuring surface displacements along the LOS directions of both ascending and descending orbits based on interferometric phases; (2) measuring surface displacements along the azimuth directions of both the ascending and descending orbits based on the SAR amplitude data; and (3) estimating the three-dimensional (3D) surface displacement field by combining the above four independent one-dimensional displacements using the method of least squares and Helmert variance component estimation. We apply the method to infer the 3D surface displacement field caused by the 2003 Bam, Iran, earthquake. The results reveal that in the northern part of Bam the ground surface experienced both subsidence and southwestward horizontal movement, while in the southern part uplift and southeastward horizontal movement occurred. The displacement field thus determined matches the location of the fault very well with the maximal displacements reaching 22, 40, and 30 cm, respectively in the up, northing and easting directions. Finally, we compare the 3D displacement field with that simulated from the Okada model. The results demonstrate that the method presented here can be used to generate reliable and highly accurate 3D surface displacement fields.

InSAR, amplitude matching, azimuth offset, three-dimensional surface displacement, Bam earthquake

Citation: Hu J, Li Z W, Zhu J J, et al. Inferring three-dimensional surface displacement field by combining SAR interferometric phase and amplitude information of ascending and descending orbits. Sci China Earth Sci, 2010, 53: 550–560, doi: 10.1007/s11430-010-0023-1

Interferometric Synthetic Aperture Radar (InSAR) has attracted the attention of the research communities of geodesy and geophysics in recent years. The advantages of InSAR, e.g., wide spatial coverage, high spatial resolution, competitive accuracy and no need for field work, make it one of the best methods for measuring co-seismic surface displacements. In 1993, Massonnet et al. [1] first estimated the displacement field caused by the Lands earthquake (28 June 1992) from the ERS-1 satellite SAR images. The results agreed very well with those obtained from GPS measurements. Since then, InSAR has been used widely for studying ground deformations associated earthquakes. However, in most studies only single-orbit SAR phase data are exploited, and this could only provide information on one-dimensional surface displacements along the LOS of the radar instead of the three-dimensional (3D) surface displacements desired for earthquake studies [2]. Some methods have been proposed to solve the problem. Wright et al. [3] resolved the 3D co-seismic surface displacements of the Nenana Mountain earthquake (23 October 2002) by com-

*Corresponding author (email: zwli@mail.csu.edu.cn)

bining interferograms acquired in four different viewing geometries. Gudmundsson et al. [4] created 3D surface motion maps of Southwest Iceland by fusing InSAR and GPS data. Fialko et al. [5] used radar image azimuth offsets and interferometric phases in deriving a 3D co-seismic surface displacement map of the 1999 M_W=7.1 Hector Mine earthquake. In China, Sun et al. [6] estimated the 3D co-seismic displacements of the 2003 Bam earthquake by combining the Okada model and ASAR data from both ascending and descending orbits. The amplitude matching method, first proposed by Michel and Avouac [7] in the study of the Landers earthquake, can estimate surface displacements in both range and azimuth directions. Although its accuracy is not as good as that of InSAR, the amplitude matching method can better resist the effects of decorrelation and can provide information on the azimuth displacements that are not measurable by InSAR. The amplitude matching method is especially suitable for monitoring large displacement fields caused by earthquakes.

On 26 December 2003, an M_W=6.5 earthquake occurred in Bam City, Iran. The flat terrain, dry climate condition, and sparse vegetable distribution in Bam make it an ideal spot for radar interferometry experiments. We therefore choose this earthquake as our research focus. Iran is located between the Arabian and the Eurasian plates, and has experienced sharp shortening as a result of the convergence of the two plates [8]. Bam is located in the southeast of Iran, 50 km east of the Gowk fault (Figure 1). Three M_W>6 earthquakes have occurred along the Gowk fault in the past 20 years, but no earthquake up to the magnitude of the 2003 one had occurred in Bam in the past 2000 years [6]. It is fortunate that the earthquake was imaged by the ENVISAT satellite from both the ascending and descending orbits. This offers a great opportunity to study the co-seismic displacements and the source parameters of the earthquake with the data.

Considering that the Bam earthquake has caused great surface displacements and no other suitable data, e.g., GPS and leveling, are available for this study, we integrate InSAR and the amplitude matching methods to study the surface displacements induced by the earthquake from both the ascending and descending SAR images. First, we estimate the co-seismic displacements along the two different LOS directions of the ascending and descending orbits with interferometric phases. Second, we measure the co-seismic displacements along the two different azimuth directions of the ascending and descending orbits with pre- and post-seismic SAR amplitude data. Finally, the method of least squares and Helmert variance component estimation are applied to combine the above four independent displacement vectors to estimate the complete three-dimensional, i.e., the up, northing and easting, surface displacement

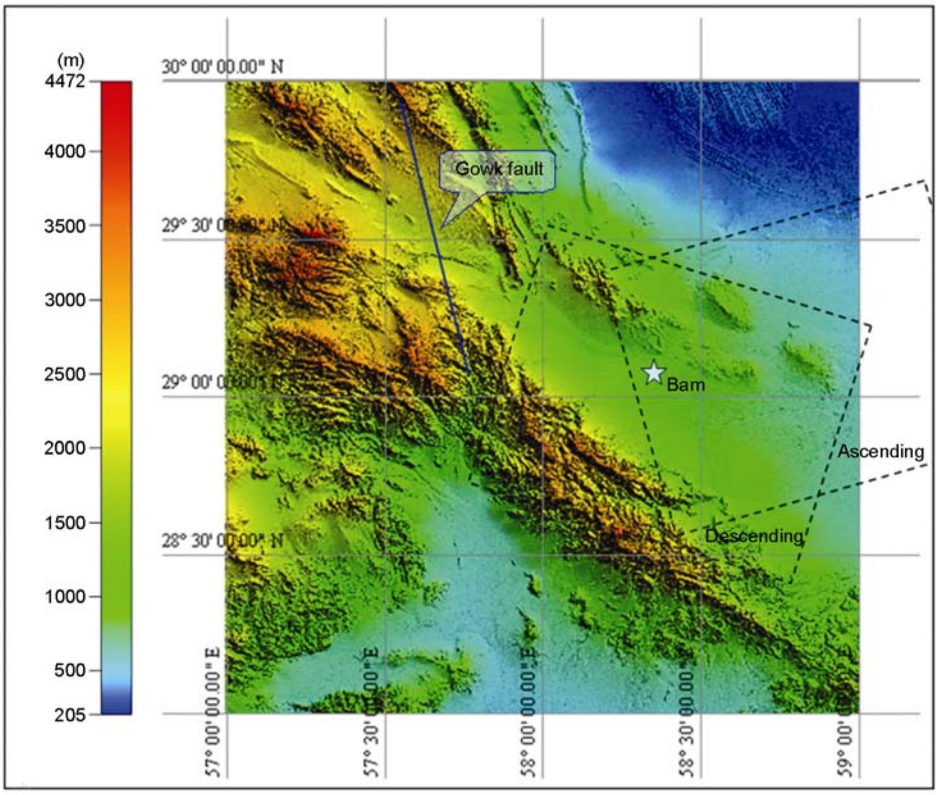

Figure 1 Shaded relief map of Bam, Iran and the frames of the ascending and descending ASAR images used for the study. The star represents the position of the epicenter. The blue line represents the Gowk fault. The interferogram in the descending orbit covers the whole area affected by the earthquake while that in the ascending orbit covers only the right half of the area. The topographic map is the conjunction of four 1°×1° SRTM data patches.

components caused by the Bam earthquake.

Concerning the Bam earthquake, Fialko et al. [9] and Funning et al. [10] have respectively done similar research in 2005. In this paper, the Helmert variance component estimation is introduced for the first time to combine the displacement vectors in different directions for improving the estimation accuracy of the 3D displacement fields. The approach of inferring three-dimensional surface displacement field by combining SAR interferometric phase and amplitude data of both ascending and descending orbits is also discussed in detail. Finally, we compare the estimated 3D displacement field with that simulated from the Okada model [11]. The results demonstrate that the method presented in the paper can be used to derive highly accurate 3D surface displacement fields caused by earthquakes.

1 3D co-seismic surface displacement field of Bam earthquake derived from SAR data

1.1 Determination of co-seismic displacements along the LOS directions from SAR interferometric phases

The European Space Agency (ESA) provided seven ENVISAT ASAR images that are related to the Bam earthquake, among which three are in the ascending orbit (one for pre-seismic and two for post-seismic) and four in the descending orbit (two for pre- and two for post-seismic). In this study, two pairs of images in ascending and descending orbits respectively are chosen for interferometric analysis based on their baselines (Table 1).

The ENVISAT satellite was launched in 2003 with a C band SAR sensor onboard. The incident angle of the sensor ranges from 15° to 45° and the satellite revisit period is 35 days. The standard SAR image covers a region of 100 km×100 km with spatial resolutions of 4 m in azimuth and 20 m in range directions [12]. GAMMA software is used to process the SAR data. For each pixel in an interferogram, its interferometric phase $\Delta\varphi$ can be written as:

$$\Delta\varphi = k\cdot 2\pi + \Delta\varphi_{\text{defo}} + \Delta\varphi_{\text{topo}} + \Delta\varphi_{\text{flat}} + \Delta\varphi_{\text{atmo}} + \Delta\varphi_{\text{noise}}, \quad (1)$$

where k is the integer ambiguity; $\Delta\varphi_{\text{defo}}$ is the phase of surface deformation; $\Delta\varphi_{\text{topo}}$ is the topographic phase; $\Delta\varphi_{\text{flat}}$ is the flat-earth phase; $\Delta\varphi_{\text{atmo}}$ is the atmospheric phase; and $\Delta\varphi_{\text{noise}}$ is the phase noise.

The ascending and descending images are processed following the procedure of co-registration, resampling, interferogram formation, and flat-earth phase removal. Precision orbits provided by the Delft University of Technology are adopted in the process to improve the accuracy of image co-registration and flat-earth phases removal [13]. Multi-looking operation with 10 pixels in azimuth and 2 pixels in range is applied to reduce the phase noise. This results in a final spatial resolution of 40 m×40 m for each interferogram. The improved Goldstein filter [14] is applied to filter the interferograms for reducing the phase noise further. As the climate condition in Bam is very dry and the atmospheric effect is subtle, we choose to ignore $\Delta\varphi_{\text{atmo}}$ as the other researchers have done [9, 10]. The phases are then unwrapped with the branch-cut algorithm [15] to determine the integer ambiguity k. At this stage, only $\Delta\varphi_{\text{defo}}$, $\Delta\varphi_{\text{topo}}$ and part of the phase noise remain in $\Delta\varphi$.

Subtracting $\Delta\varphi_{\text{topo}}$ from $\Delta\varphi$ can be achieved with the two-pass, three-pass or four-pass approaches. In the two-pass approach, the topographic phases are simulated from external DEM and removed from the interferometric phases. As the approach needs the least SAR images, it is commonly used in practice. The accuracy of this approach is primarily dependent on the accuracy of the external DEM δh and the perpendicular baseline $B_\perp$ [16]:

$$\delta R = \frac{\delta h}{R\sin\theta} B_\perp, \quad (2)$$

where θ is the radar incident angle; and R is the slant range. Considering the perpendicular baselines of the two interferograms chosen in this study are both very small (Table 1), we apply the two-pass approach to remove $\Delta\varphi_{\text{topo}}$. The SRTM data with spatial resolution of about 90 m×90 m is used as the external DEM. The nominal elevation accuracy of the SRTM data is 16 m [17]. This can cause 0.1 and 0.03 mm deformation errors for the ascending and descending interferograms respectively based on eq. (2). The errors are therefore negligible.

To match the SRTM data to the SAR images, we transform the SRTM data from WGS 84 to the SAR coordinate system. Then we interpolate the SRTM data to the spatial resolution of SAR interferogram and simulate the topographic phases from the interpolated SRTM data. The differential interferograms can be obtained by subtracting the simulated topographic phases from the original interferograms. Figure 2 shows the differential interferograms from the ascending and descending orbits. Finally, the differential interferograms are transformed into surface displacements and geocoded back to WGS 84 coordinate system. The surface displacements caused by the Bam earthquake have thus

Table 1 SAR data used in the study

Orbit	Master (pre-seismic)	Slave (post-seismic)	Time interval	Perpendicular baseline
Ascending	16 November 2003	29 February 2004	105 days	2 m
Descending	3 December 2003	11 February 2004	70 days	0.6 m

been created. Figure 3 shows the surface displacements for the ascending and descending orbits, respectively. In this study, the accuracy of the displacements can reach the level of one centimeter because of the short time interval and good coherence between the SAR images [10]. However, it is noteworthy that the displacements are the projections of the real 3D surface deformation onto the LOS directions of the ascending and descending orbits. We can find in Figure 3 that great differences exist in the displacement fields determined from data of the ascending and descending orbits. Therefore, it is concluded that the single orbit interferometric SAR data cannot reveal the exact surface deformation.

1.2 Determination of co-seismic displacements along azimuth directions from SAR amplitude data

SAR images contain phase as well as amplitude information. In the last section, we have applied the SAR phase information (interferometric phases) to measure the co-seismic displacements along the LOS directions. In this section, we will use the SAR amplitude information and the method of amplitude matching to estimate the co-seismic displacements along the azimuth directions. The data listed in Table 1 will be used again for the study. As a result of surface deformation and satellite orbit separation, the post-seismic

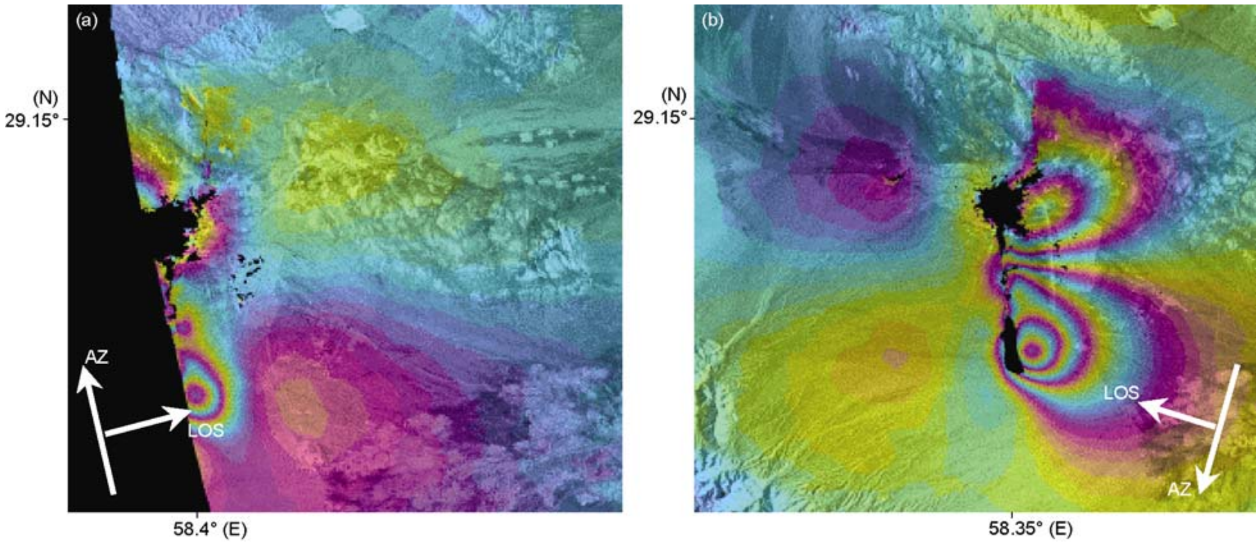

Figure 2 Co-seismic interferograms of the Bam earthquake from ascending (a) and descending (b) orbits. Each interferometric fringe represents about 8 cm of relative surface displacements. The black region in (b) is the rupture zone of the earthquake, which reveals the approximate position of the fault [8, 18]. The rupture in this region is so great that serious decorrelation occurs, which makes interferometric measurements in the region impossible [19]. LOS represents the line of sight direction, and AZ represents the azimuth direction, i.e., the projection of satellite flight path onto ground; the same below.

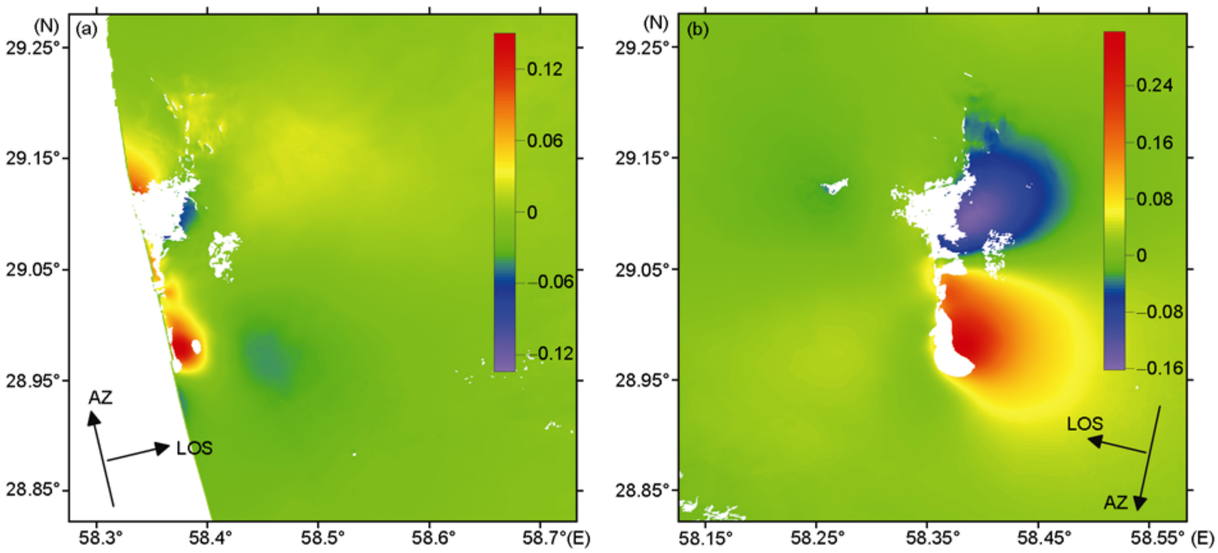

Figure 3 Surface displacements along the LOS directions of ascending (a) and descending (b) orbits caused by the Bam earthquake. The maximum displacements from the ascending and descending orbit measurements are about 0.14 and 0.30 m, respectively.

SAR amplitude image will have pixel-by-pixel shift with respect to the pre-seismic image. The shifts in the directions of azimuth and range are named as AZimuth Offset (AZO) and Range Offset (RO), respectively. The accuracy of estimating the offsets with amplitude matching can reach 1/50 of a pixel, equivalent to 7.5 cm in azimuth direction and 14 cm in range direction for ASAR data [20]. It is obvious that the accuracy is much lower than that of SAR interferometry. Therefore, the amplitude matching method is not suitable for monitoring small surface deformations. However, the method is very useful for measuring large surface deformations caused by earthquakes, as it can resist the effects of decorrelation caused by large deformation on one hand and monitor the deformation in the azimuth direction that is not measurable by InSAR on the other. Michel and Avouac [7] demonstrated in the study of the Landers earthquake that the method of amplitude matching can monitor surface displacements caused by earthquakes with an accuracy of centimeter level. We will use the method of amplitude matching in this study considering that the displacements caused by the Bam earthquake are large and that the method is supplementary to InSAR. As the accuracy of range offsets determined by amplitude matching is lower than that of azimuth offsets, we will only use the offsets in the azimuth direction.

The pre- and post-seismic SAR amplitude images are processed with coarse co-registration first. The preliminary offsets in the azimuth directions of the ascending and descending orbits are 12090 and −6183 pixels, respectively. The offsets are caused mostly by satellite orbit separation. Based on the results, fine co-registration is carried out to estimate the total azimuth offset R_{offset} at each pixel, which includes two parts:

$$R_{\text{offset}}=R_{\text{orbit}}+R_{\text{AZO}}, \tag{3}$$

where R_{orbit} represents the offset induced by the satellite orbit separation and R_{AZO} the offset caused by surface displacement along the azimuth direction (referred to as azimuth displacement hereinafter). Figure 4(a) and (c) show the total azimuth offsets for the ascending and descending orbits, respectively. It is found that the azimuth displacements in the dashed rectangle are distinctly visible although the orbit offsets are dominant in the results. To separate R_{AZO} from R_{offset}, R_{orbit} must be estimated and eliminated.

As the displacement field caused by the Bam earthquake is only concentrated in the area near the Bam City and dis-

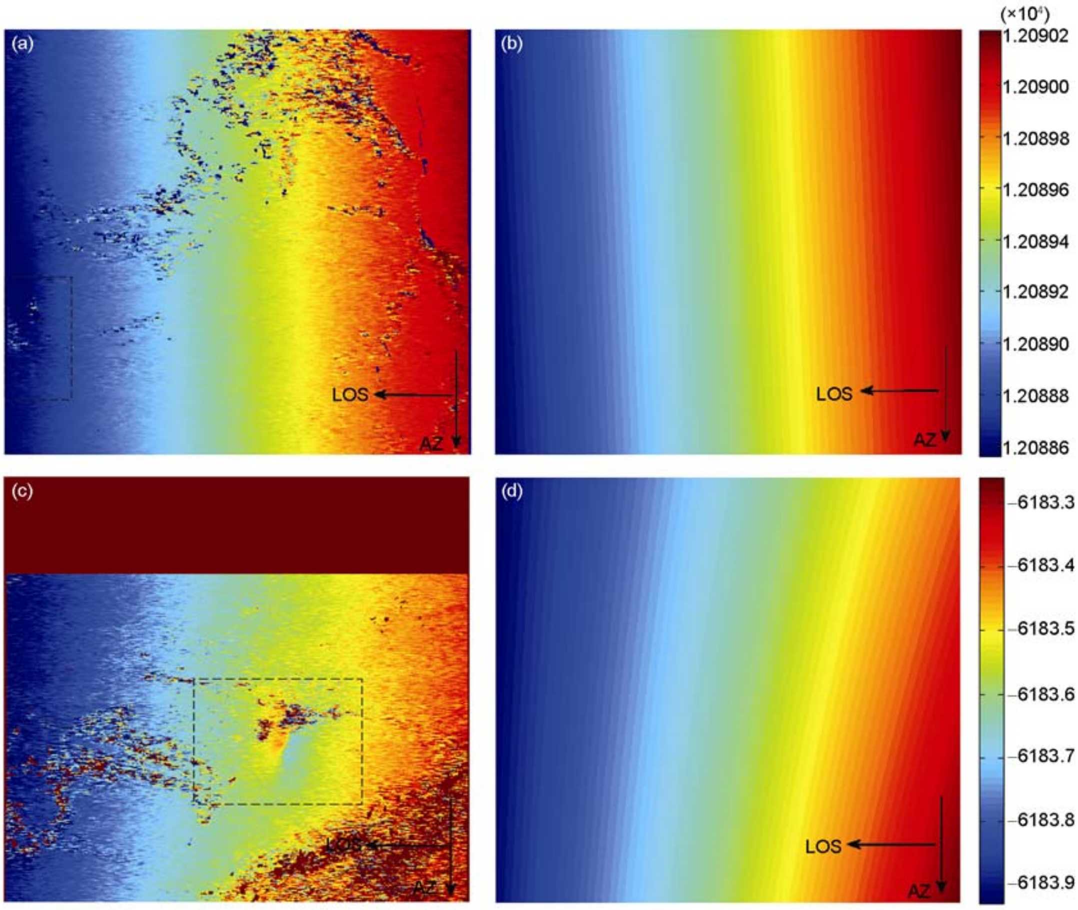

Figure 4 (a) and (c) are total azimuth offsets for the ascending and descending orbits, and (b) and (d) are orbit offsets modeled by biquadratic polynomials for the ascending and descending orbits (units pixel).

placements decreased almost to zero in the area beyond 25 km from the epicenter [21], we can safely assume that $R_{\rm offset}$ estimated in the relatively stable areas only contain the orbit offset $R_{\rm orbit}$. A biquadratic polynomial model is established to model $R_{\rm orbit}$ by utilizing the offsets estimated in the stable areas [22]:

$$R_{\rm orbit} = a_0 + a_1 x + a_2 y + a_3 xy + a_4 x^2 + a_5 y^2, \tag{4}$$

where x and y are the coordinates in the SAR coordinate system; a_i (i=0, 1, ..., 5) are the polynomial coefficients that can be estimated with the observation samples and the method of least squares. Then, the model can be used to infer the orbit offset $R_{\rm orbit}$ in the area where deformation occurred. The $R_{\rm orbit}$ results thus obtained for the ascending and descending orbits are shown in Figure 4(b) and (d), respectively. The azimuth displacements $R_{\rm AZO}$ can then be obtained by differentiating $R_{\rm orbit}$ from $R_{\rm offset}$. Figure 5 shows the geocoded $R_{\rm AZO}$ for the ascending and descending orbits.

1.3 Determination of 3D co-seismic displacement field

We suppose that the 3D co-seismic displacement field of the Bam earthquake can be represented by three components, r_U, r_N and r_E, respectively in the up, northing and easting directions. Four independent displacement vectors, i.e., the LOS displacement vector from the ascending orbit measurements, the LOS displacement vector from the descending orbit measurements, the azimuth displacement vector of the ascending orbit, and the azimuth displacement vector of the descending orbit, have been estimated in the previous two sections. We denote these vectors as $R^A_{\rm LOS}$, $R^D_{\rm LOS}$, $R^A_{\rm AZO}$ and $R^D_{\rm AZO}$, respectively.

Observation equation can be constructed according to the geometry of the SAR image acquisitions (Figure 6) [3, 5]:

$$v = U \cdot r - R, \tag{5}$$

where $R = \begin{bmatrix} R^A_{\rm LOS} \\ R^D_{\rm LOS} \\ R^A_{\rm AZO} \\ R^D_{\rm AZO} \end{bmatrix}$; $r = \begin{bmatrix} r_U \\ r_N \\ r_E \end{bmatrix}$; $v = \begin{bmatrix} v^A_{\rm LOS} \\ v^D_{\rm LOS} \\ v^A_{\rm AZO} \\ v^D_{\rm AZO} \end{bmatrix}$ is the corresponding observation error vector; and

$$U = \begin{bmatrix} \cos\theta_A & -\cos\left(\alpha_A - \frac{3\pi}{2}\right)\sin\theta_A & -\sin\left(\alpha_A - \frac{3\pi}{2}\right)\sin\theta_A \\ \cos\theta_D & -\cos\left(\alpha_D - \frac{3\pi}{2}\right)\sin\theta_D & -\sin\left(\alpha_D - \frac{3\pi}{2}\right)\sin\theta_D \\ 0 & \sin\left(\alpha_A - \frac{3\pi}{2}\right) & -\cos\left(\alpha_A - \frac{3\pi}{2}\right) \\ 0 & \sin\left(\alpha_D - \frac{3\pi}{2}\right) & -\cos\left(\alpha_D - \frac{3\pi}{2}\right) \end{bmatrix}$$

is the projection matrix, where α_A and α_D are the azimuth angles for the ascending and descending orbits, 346.5° and 193.5° respectively for this study; θ_A and α_D are the pixel-based radar incident angles for the ascending and descending orbits, respectively. As the displacement field caused by the Bam earthquake only covers an area of about 30 km^2 and the terrain in the area is very flat, the variations of the radar incident angle between pixels within the area did not exceed 1°. We therefore assume that the radar incident angles of all the pixels are the same and are equal to

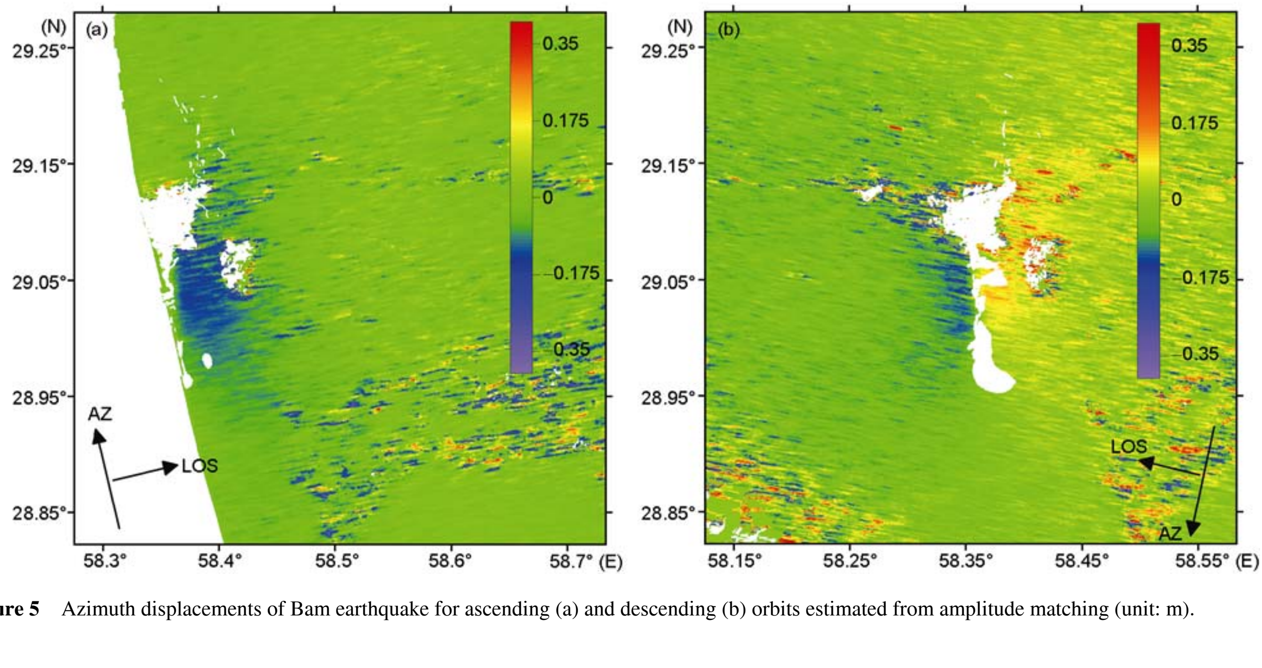

Figure 5 Azimuth displacements of Bam earthquake for ascending (a) and descending (b) orbits estimated from amplitude matching (unit: m).

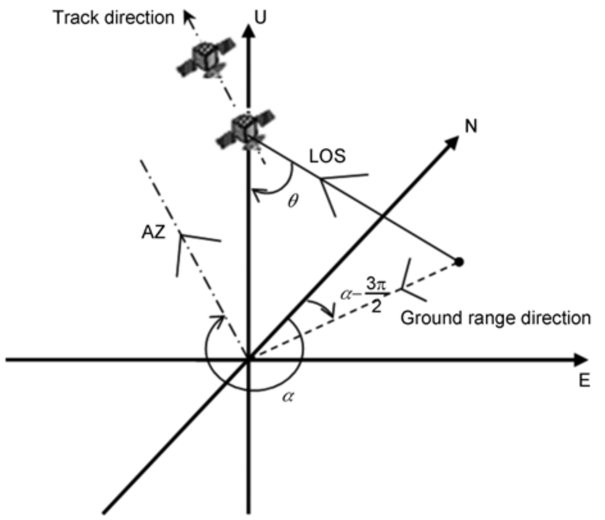

Figure 6 3D geometry of SAR image acquisition. α represents the azimuth angle, i.e., the angle between the north and the track direction (clockwise). The ground range direction is the projection of the LOS onto ground. α–3π/2 is the angle between the north and the ground range direction. The arrows indicate the directions of positive displacement.

that of the center pixel in the area, i.e., θ_A=21.3° and θ_D=23.7°. Experiments have verified that the errors from this assumption are at the sub-millimeter level and do not affect significantly the accuracy of the 3D co-seismic surface displacement estimation [5, 6].

For each pixel, there are three unknown parameters and four observations in eq. (5). Under the condition of weighted least squares, i.e., $v^{\mathrm{T}}Pv$ is minimum, the 3D co-seismic surface displacement field can be determined by

$$\hat{r} = (U^{\mathrm{T}}PU)^{-1}U^{\mathrm{T}}PR, \tag{6}$$

where P represents the weight matrix of the observations. In earlier research, P has been commonly assumed an identity matrix, i.e., disregarding the accuracies of the observations. As the accuracy of SAR interferometry is much higher than that of amplitude matching, equal weighting of the observations will certainly affect the accuracy of the 3D displacement field estimation.

To resolve this problem, we divide the observations into two classes according to their accuracies, i.e. $R_1 = [R_{\mathrm{LOS}}^A, R_{\mathrm{LOS}}^D]^{\mathrm{T}}$ and $R_2 = [R_{\mathrm{AZO}}^A, R_{\mathrm{AZO}}^D]^{\mathrm{T}}$. Their corresponding weight matrices are P_1 and P_2 respectively, where $P_1 \neq P_2$. Eq. (5) can then be modified into

$$\begin{cases} v_1 = U_1 \cdot r - R_1, \\ v_2 = U_2 \cdot r - R_2, \end{cases} \tag{7}$$

where $v_1 = [v_{\mathrm{LOS}}^A, v_{\mathrm{LOS}}^D]^{\mathrm{T}}$, $v_2 = [v_{\mathrm{AZO}}^A, v_{\mathrm{AZO}}^D]^{\mathrm{T}}$; and

$$U_1 = \begin{bmatrix} \cos\theta_A & -\cos\left(\alpha_A - \frac{3\pi}{2}\right)\sin\theta_A & -\sin\left(\alpha_A - \frac{3\pi}{2}\right)\sin\theta_A \\ \cos\theta_D & -\cos\left(\alpha_D - \frac{3\pi}{2}\right)\sin\theta_D & -\sin\left(\alpha_D - \frac{3\pi}{2}\right)\sin\theta_D \end{bmatrix},$$

$$U_2 = \begin{bmatrix} 0 & \sin\left(\alpha_A - \frac{3\pi}{2}\right) & -\cos\left(\alpha_A - \frac{3\pi}{2}\right) \\ 0 & \sin\left(\alpha_D - \frac{3\pi}{2}\right) & -\cos\left(\alpha_D - \frac{3\pi}{2}\right) \end{bmatrix}.$$

As the prior variances of R_1 and R_2 can hardly be estimated accurately, weight matrices P_1 and P_2 cannot be determined accurately before the adjustment. The method of Helmert variance component estimation is introduced here to iteratively determine P_1 and P_2. We start with identity matrices as the initial values of P_1 and P_2, and estimate the 3D surface displacements with the method of least squares. According to the Helmert variance component estimation [23], we can get

$$\hat{\theta} = S^{-1}W_\theta, \tag{8}$$

where $\hat{\theta} = [\hat{\sigma}_{01}^2, \hat{\sigma}_{02}^2]^{\mathrm{T}}$ are the estimates of the unit variances (or variance factors) for R_1 and R_2; $W_\theta = [v_1^{\mathrm{T}}P_1v_1,\ v_2^{\mathrm{T}}P_2v_2]^{\mathrm{T}}$; and

$$S = \begin{bmatrix} 2-2\mathrm{tr}((U^{\mathrm{T}}PU)^{-1}U_1^{\mathrm{T}}P_1U_1) + \mathrm{tr}((U^{\mathrm{T}}PU)^{-1}U_1^{\mathrm{T}}P_1U_1)^2 & \mathrm{tr}((U^{\mathrm{T}}PU)^{-1}U_1^{\mathrm{T}}P_1U_1 \cdot (U^{\mathrm{T}}PU)^{-1}U_2^{\mathrm{T}}P_2U_2) \\ \mathrm{tr}((U^{\mathrm{T}}PU)^{-1}U_1^{\mathrm{T}}P_1U_1 \cdot (U^{\mathrm{T}}PU)^{-1}U_2^{\mathrm{T}}P_2U_2) & 2-2\mathrm{tr}((U^{\mathrm{T}}PU)^{-1}U_2^{\mathrm{T}}P_2U_2) + \mathrm{tr}((U^{\mathrm{T}}PU)^{-1}U_2^{\mathrm{T}}P_2U_2)^2 \end{bmatrix}.$$

The weight matrices can be determined following

$$\hat{P}_i = \frac{1}{\hat{\sigma}_{0i}^2 P_i^{-1}}, \quad (i=1, 2). \tag{9}$$

The weight matrices are replaced by the new ones in eqs. (6)–(9) for iterative computation, i.e., least squares adjustment-Helmert variance component estimation-updating weight and least squares adjustment, until $\hat{\sigma}_{01}^2 = \hat{\sigma}_{02}^2$. When the final weight matrices $\hat{P}_1$ and $\hat{P}_2$ are determined, the final 3D surface displacements can be estimated with eq. (6).

Figure 7 shows the 3D co-seismic surface displacement field caused by the Bam earthquake estimated with the above methods. It can be seen from Figure 7(a) that the surface in the northern part of Bam experienced some subsidence, while that in the southern part some uplift. Figure 7(b) and (c) show that southwestward horizontal movement occurred in the northern part of Bam, whereas southeastward horizontal movement in the southern part. Al-

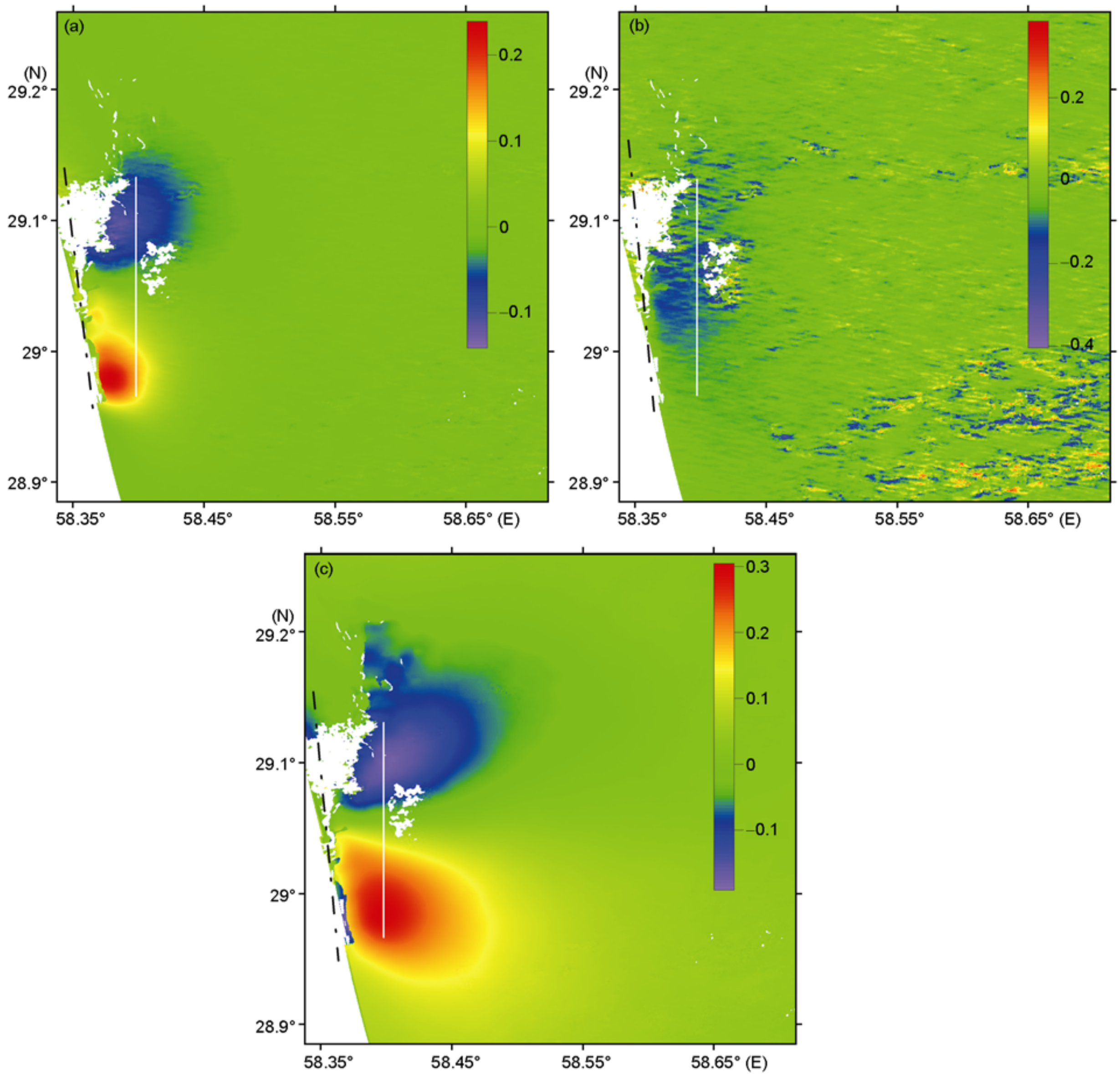

Figure 7 3D co-seismic surface displacement field of the Bam earthquake estimated from SAR data: up component (a), northing component (b), and easting component (c). The maximum displacements along the up, northing and easting directions are 0.22, 0.40 and 0.30 m, respectively. The black dashed lines represent the projection of the fault [8, 10, 18] and the white solid line marks the location of a profile that will be extracted for further analysis (unit: m).

though the left part of the surface displacement field cannot be determined as it is not covered by the SAR images, the right part of the surface displacement field has been successfully retrieved. According to refs. [8, 10, 18], the displacement components in the up, northing and easting directions agree very well with the location of the fault. This demonstrates that the method of combining SAR interferometric phase and amplitude information can determine accurately surface displacement fields. However, the results also show that in the northing direction there is still some noise (Figure 7(b)), while in the up and easting directions the displacement results are very clean (Figure 7(a) and (c)). The reason for this phenomenon is that the ENVISAT satellite flies nearly in the north-south direction (with a deviation of about 12°), which makes SAR interferometry insensitive to the surface displacements in the north direction. Therefore, the surface displacement field along the north direction is mostly retrieved from the azimuth offsets that have some intrinsic noises (see Figure 5).

2 3D co-seismic surface displacement field of Bam earthquake simulated from Okada model

To validate the 3D co-seismic surface displacement field estimated from SAR data as presented in the last section, we

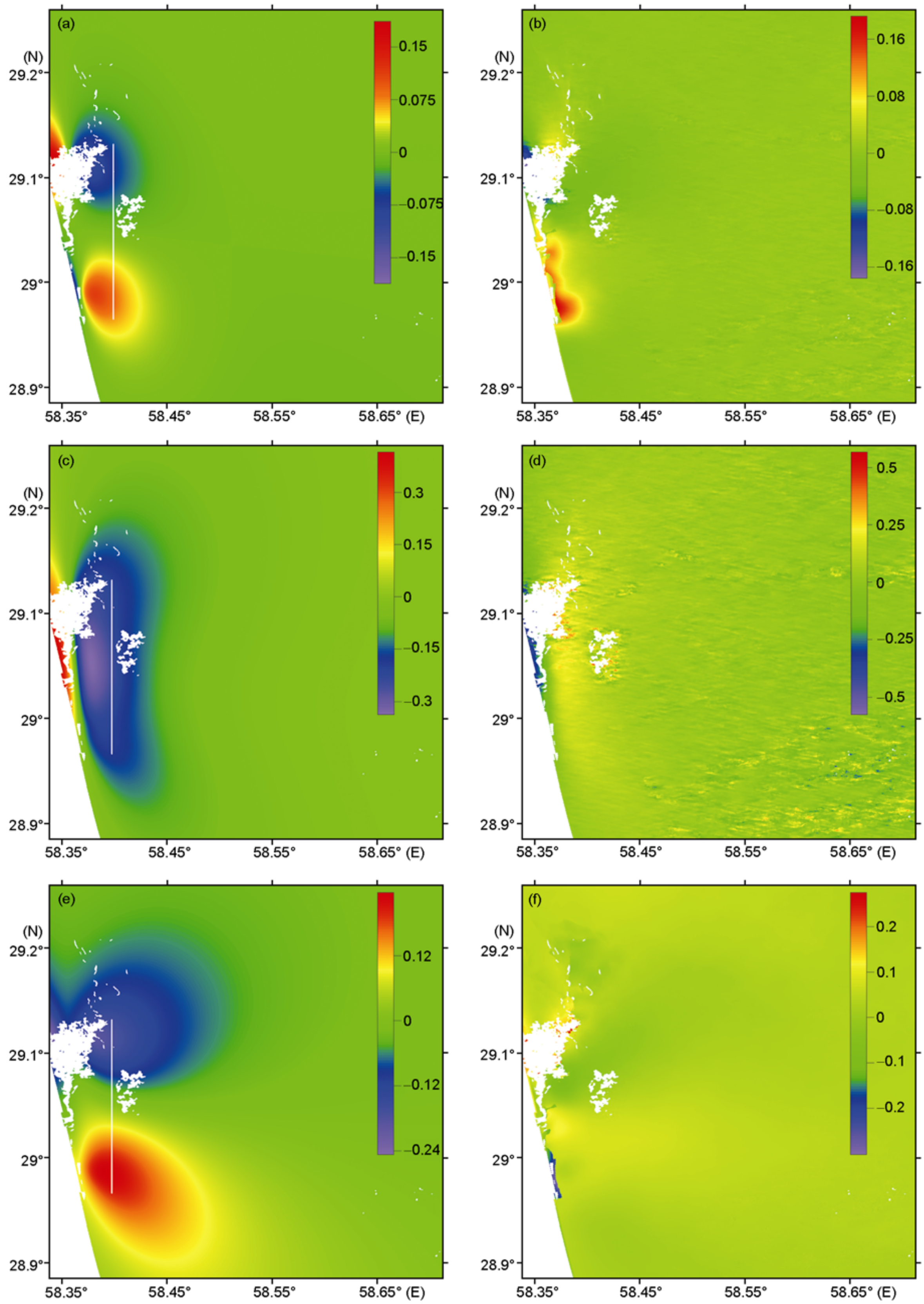

Figure 8 3D surface displacement fields of the Bam earthquake simulated from the Okada model and their differences with respect to those estimated from SAR data. (a), (c), and (e) are the simulated surface displacement components in the up, northing and easting directions, respectively. (b), (d), and (f) are the corresponding residuals between the simulated and the measured displacement values (unit: m).

will simulate the 3D co-seismic surface displacement field based on the Okada model [11] and compare the two independent surface displacement fields.

Since the Bam earthquake, many geophysicists have worked on determining the source parameters of the earthquake [8, 10, 18, 24, 25]. After comparative analysis, we choose the source parameters with a single fault given by Funning et al. [10] for the Okada model (Table 2). Figure 8(a), (c), and (e) shows the 3D displacement field of the Bam earthquake simulated from the model. Figure 8(b), (d), and (f) shows the residuals between the displacement field simulated from the Okada model and that estimated by combining SAR interferometric phase and amplitude information along the up, northing, and easting directions, respectively. The two sets of results agree with each other very well although some residuals still exist. The results are also compared in Figure 9 along a profile that is almost parallel to the fault. It is seen that the displacements estimated by the SAR data in the up and easting directions are smooth and match well with those simulated from Okada model (with deviations of only several centimeters), whereas the estimated results in the northing direction are much more noisy. The results demonstrate that the SAR interferometric phase can provide much more accurate displacement information than SAR amplitude. Despite the lower accuracy in the northing direction, the deviation of about 5 cm in the direction as shown in Figure 9(b) is still within the accuracy of the azimuth offset method (i.e., 7.5 cm).

Although the general trends of the 3D co-seismic displacement fields estimated from SAR data and simulated from the Okada model are almost the same, some notable differences between them do exist. There are several reasons for the differences. First, the simulated displacement field cannot fully characterize the real one. Second, the accuracy of estimating the azimuth offset from SAR amplitude matching is not high enough. Finally, the phases in the area of low coherence affect the estimation of the displacements.

3 Conclusions

One of the main limitations of InSAR is that only one dimensional surface displacements along the radar LOS direction can be measured [21] and the displacements in one direction cannot fully reflect the surface deformation under many circumstances. This paper has presented a method for

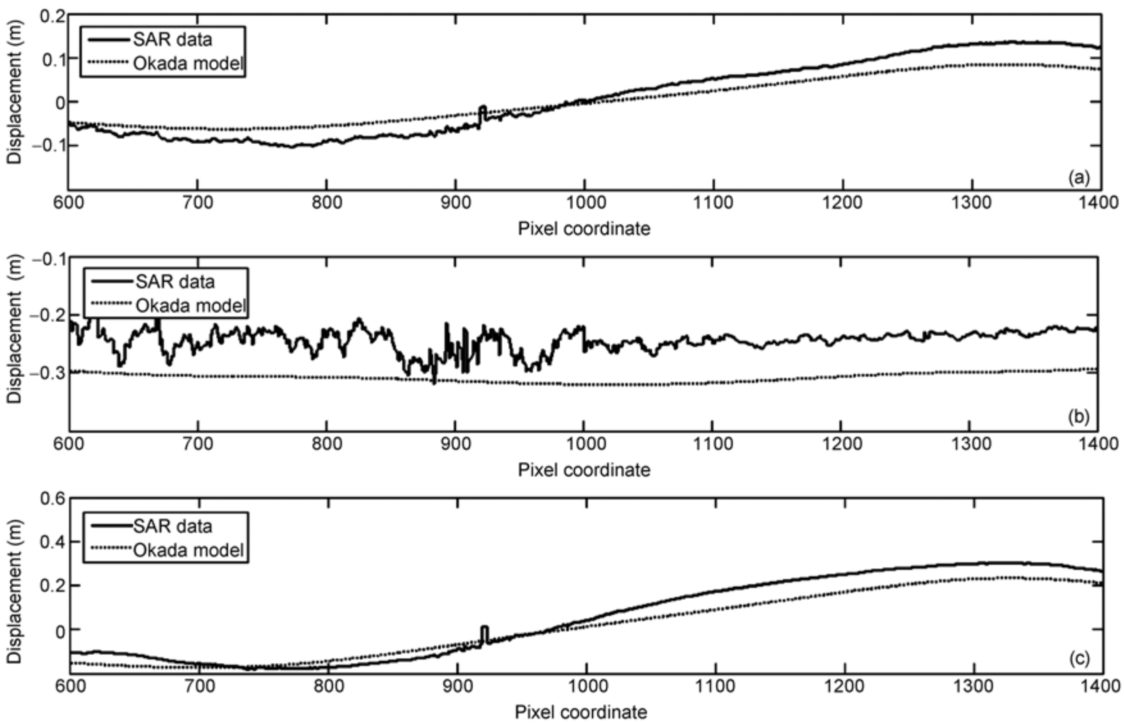

Figure 9 Comparison between the displacements determined from the SAR data and from the Okada model, up component (a), northing component (b), and easting component (c) along the profile marked in Figures 7 and 8.

Table 2 The source parameters of the Bam earthquake [10]

Longitude	Latitude	Depth (km)	Strike	Dip	Rake	Slip (m)	Length (km)	Width (km)
29.037°E	58.353°N	5.2	354.4°	83.8°	−177.6°	2.20	12.0	8.1

inferring 3D surface displacement fields from combining SAR interferometric phase and amplitude information of ascending and descending orbits. The method makes full use of the deformation information in data from both ascending and descending orbits.

The 3D co-seismic surface displacement field caused by the Bam, Iran, earthquake has been inferred from the pre- and post-seismic ENVISAT ASAR images of the ascending and descending orbits. To demonstrate the accuracy and reliability of the method, we compare the 3D co-seismic surface displacement field thus obtained with that simulated from the Okada model. The two sets of results compare well with each other.

The method presented here is not only suitable for integrating data from ascending and descending orbits, but should also be useful for integrating SAR data from different flight tracks, satellites and radar incident angles. As the accuracy of estimating offsets from ENVISAT ASAR amplitude images is not very high, due mainly to the low spatial resolution of ASAR data [20], the method is only suitable for measuring large displacements caused by, e.g., earthquakes, volcanoes, and glacier movement. With the recent release of the 3 m×3 m or even 1 m×1 m resolution TerraSAR and COSMO-SkyMed SAR data, it is possible to measure finer scale 3D surface displacements by using the method presented.

We are grateful to the European Space Agency (ESA) for supplying the SAR data, and thank Dr. Charles L. Werner and Dr. Urs Wegmuller for their help in using GAMMA software, and thank Dr. Hua Wang of Wuhan University for his advice in the offset method. We also thank the anonymous reviewers for their constructive modification suggestions to the paper. This work was supported by National Natural Science Foundation of China (Grant Nos. 40774003 and 40974006), National High Technology Research and Development Program of China (Grant No. 2006AA12Z156), Program for New Century Excellent Talents in Universities (Grant No. NCET-08-0570), the Project of Western China 1:50000 Topography Mapping, the Project of Doctoral Dissertation Innovation (Grant No. 2008yb046) and the Sustentation Fund of the Excellent Doctoral Dissertation (Grant No. 1960- 71131100022) of Central South University.

1 Massonnet D, Rossi M, Carmona C, et al. The displacement field of the Landers earthquake mapped by radar interferometry. Nature, 1993, 364: 138–142
2 Ding X L, Liu G X, Li Z W, et al. Ground subsidence monitoring in Hong Kong with satellite SAR interferometry. Photogramm Eng Remote Sens, 2004, 70: 1151–1156
3 Wright T J, Parsons B E, Lu Z. Toward mapping surface deformation in three dimensions using InSAR. Geophys Res Lett, 2004, 31: L01607
4 Gudmundsson S, Sigmundsson F. Three-dimensional surface motion maps estimated from combined interferometric synthetic aperture radar and GPS data. J Geophys Res, 2002, 107(B10): 1–14
5 Fialko Y, Simons M, Agnew D. The complete (3-D) surface displacement field in the epicentral area of the 1999 M_W7.1 Hector Mine earthquake, California, from space geodetic observations. Geophys Res Lett, 2001, 28: 3063–3066
6 Sun J B, Liang F, Xu X W, et al. 3D co-seismic deformation field of the Bam earthquake (M_W 6.5) from ascending and descending pass ASAR radar interfeometry (in Chinese). J Remote Sens, 2006, 10: 489–496
7 Michel R, Avouac J. Measuring near field coseismic displacements from SAR images: Application to the Landers earthquake. Geophys Res Lett, 1999, 26: 3017–3020
8 Perski Z, Hanssen R. The interperetation of Bam fault kinematics using ENVISAT SAR interferometric data. Fringe 2005 Workshop, Frascati, Italy, 2005. 1–6
9 Fialko Y, Sandwell D, Simons M, et al. Three-dimensional deformation caused by the Bam, Iran, earthquake and the origin of shallow slip deficit. Nature, 2005, 435: 295–299
10 Funning G J, Parsons B, Wright T J, et al. Surface displacements and source parameters of the 2003 Bam (Iran) earthquake from Envisat advanced synthetic aperture radar imagery. J Geophys Res, 2005, 110: B09406
11 Okada Y. Surface deformation due to shear and tensile faults in a half-space. Bull Seismol Soc Amer, 1985, 75: 1135–1154
12 European Space Agency. ASAR Product Handbook. Version 2.2. European Space Agency, 2007
13 Scharoo R, Visser P. Precise orbit determination and gravity field improvement for the ERS satellites. J Geophys Res, 1998, 103: 8113–8127
14 Li Z W, Ding X L, Huang C, et al. Filtering method for radar interferogram with strong noise. Int J Remote Sens, 2006, 27: 2991–3000
15 Goldstein R M, Zebker H A, Werner C L. Satellite radar interferometry: Two-dimensional phase unwrapping. Radio Sci, 1998, 23: 713–720
16 Nolan M, Fatland D R. New DEMs may stimulate significant advancements in remote sensing of soil moisture. Eos Trans AGU, 2003, 84: 233
17 Smith B, Sandwell D. Accuracy and resolution of shuttle radar topography mission data. Geophys Res Lett, 2003, 30: 1467–1470
18 Talebian M, Fielding E J, Funning G J, et al. The 2003 Bam (Iran) earthquake: Rupture of a blind strike-slip fault. Geophys Res Lett, 2004, 31: L11611
19 Fielding E J, Talebian M, Rosen P A, et al. Surface ruptures and building damage of the 2003 Bam, Iran, earthquake mapped by satellite synthetic aperture radar interferometric correlation. J Geophys Res, 2005, 110: B03302
20 Werner C, Wegmuller U, Strozzi T, et al. Precision estimation of local offsets between pairs of SAR SLCs and detected SAR images. International Geoscience and Remote Sensing Symposium, Seoul, Korea, 2005. 4803–4805
21 Xia Y. Bam earthquake: Surface deformation measurement using radar interferometry (in Chinese). Acta Seismol Sin, 2005, 27: 423–430
22 Wang H, Ge L L, Xu C J, et al. 3-D coseimic displacement field of the 2005 Kashmir earthquake inferred from satellite radar imagery. Earth Planets Space, 2007, 59: 343–349
23 Cui X Z, Yu Z C, Tao B Z, et al. General Surveying Adjustment (in Chinese). 2nd ed. Beijing: Surveying Press, 1992
24 Nakamura T, Suzuki S, Sadeghi H, et al. Source fault structure of the 2003 Bam earthquake, southeastern Iran, inferred from the aftershock distribution and its relation to the heavily damaged area: Existence of the Arg-e-Bam fault proposed. Geophys Res Lett, 2005, 32: L09308
25 Wang R, Xia Y, Grosser H, et al. The 2003 Bam (SE Iran) earthquake: Precise source parameters from satellite radar interferometry. Geophys J Int, 2004, 159: 917–922